

Nonstationary stimulated Mandel'shtam-Brillouin scattering of focused light beams under saturation conditions

N. F. Andreev, V. I. Bespalov, M. A. Dvoretiskii, and G. A. Pasmanik

Institute of Applied Physics, USSR Academy of Sciences

(Submitted 1 March 1983)

Zh. Eksp. Teor. Fiz. **85**, 1182–1191 (October 1983)

It is shown that reversal of the wave front of focused single-mode beams in nonstationary stimulated Mandel'shtam-Brillouin scattering (SMBS) in SF₆ ($p = 16$ atm) in a wide range of laser-emission energy (from 0.3 to 3 J) takes place with a high reflection coefficient ($R_W \approx 0.9-0.95$) and with high accuracy ($\chi \approx 0.95$). It was observed that the nonstationary character of the SMBS leads to a change, in the course of time, of the spatial distribution of the hypersound and laser-radiation intensities in the interior of a nonlinear medium. At sufficiently high laser radiation energy the characteristic region of its attenuation by scattering from hypersound into a secondary Stokes wave is localized near the entry to the nonlinear medium. As a result, the power of the radiation passing through the focal constriction decreases sharply with time and helps prevent optical breakdown. By coupling the investigated SMBS mirror with a two-pass neodymium amplifier it is possible to achieve with a relatively weak input signal ($W \approx 0.03$ J/cm²) a single-frequency single-mode beam with a pulse duration 33 nsec and an energy output close to the limiting value 0.12 J/cm³. The maximum radiation output energy of the two-pass amplifier is 20 J.

PACS numbers: 42.65.Cq, 42.60.He, 51.70.+f

1. INTRODUCTION

The reason for the considerable attention paid lately to stimulated Mandel'shtam-Brillouin scattering (SMBS) is that this nonlinear effect is being more extensively used in laser optics for light wave-front reversal (WFR) and to increase the output emission brightness of two-pass optical amplifiers.^{1,2} If the amplifiers and the other elements are optically inhomogeneous, the use of an SMBS mirror permits compensation of the wave-front distortion in the return pass. However, WFR in SMBS of spatially inhomogeneous (multimode) beams is accompanied by excitation of a collateral (uninverted) components whose presence prevents maximum brightness from being reached and can cause such undesirable effects as breakdown of the optical elements and others. To attain maximum radiation brightness it is therefore more convenient to use optically homogeneous amplifiers and pass single-mode beams through them.^{2,3} In this case the SMBS mirror not only affects the FWR, but serves also, by virtue of the threshold dependence of the reflection coefficient on the radiation power, as a nonlinear filter that prevents self-excitation of the amplifiers.

What is most difficult when working with single-mode light beams is to obtain high accuracy χ of the WFR and a close-to-unity reflection coefficient R_W at high excess above the SMBS threshold. The point is that SMBS in liquids is accompanied at high excess above threshold by collateral nonlinear effects that prevents the values $\chi = 1$ and $R_W = 1$ to be reached. These collateral effects do not occur as a rule in compressed gases, but the SMBS process is usually nonstationary, since the duration of the giant pulses used in the experiment is comparable with or less than the hypersound relaxation time. It is therefore important to investigate the nonstationary effects at large excesses above the SMBS threshold, i.e., in the saturation regime, when $R_W = 1$. The need for this investigation is evident also from the fact that

compressed gases are already being used as the nonlinear media of SMBS mirrors for two-pass laser systems.²

We report here such an investigation and show that large ($\sim 90-95\%$) reflection coefficients and high ($\sim 95\%$) accuracy of WFR in single-mode focused light beam is achieved for nonstationary SMBS in a wide range of beam energy (from 0.3 to 3 J). We have observed that the nonstationary character of the SMBS leads to time variation of the spatial distribution of the intensities of the hypersound and of the laser radiation in the interior of the nonlinear medium. The hypersound is initially excited near the focus of the lens, after which the region of its excitation moves counter to the incident beam. At sufficiently high laser-pulse energy the characteristic region of its attenuation due to scattering by hypersound into an opposing Stokes wave is localized near the entry into the nonlinear medium. As a result, the power of the radiation passing through the focal constriction decreases rapidly with time, thus contributing to elimination of optical breakdown and of other side effects. The combination of the investigated SMBS mirror with a two-pass neodymium amplifier has made it possible to obtain in a single-mode single-frequency beam (with pulse duration 33 nsec) a high spectral radiation brightness and a near-maximum extraction of the energy stored in the amplifiers.

2. ENERGY AND SPATIAL CHARACTERISTICS OF SMBS

The SMBS was excited in a cell 1 m long with compressed ($p = 16$ atm) SF₆ gas, into which focused (focal length $F = 1.05$ m) a single-mode neodymium-laser beam (pump) of wavelength $\lambda = 1.054$ μ m, pulse duration $\tau = 33$ nsec, and diameter and divergence (at $1/e$ level) $d_0 = 1$ mm and $\theta_0 = 6.8 \times 10^{-5}$ rad, respectively. Since the hypersound relaxation time T_2 is close to the pump-pulse duration, the SMBS process is nonstationary. Figure 1 shows the measured energy reflection coefficient $R_W = W_1/W_0$ as a func-

tion of the excess above the threshold $W_{\text{thr}} = 0.015 \text{ J}$ (curve 1). It can be seen that R_w increases rapidly as the pulse energy changes from W_{thr} to $20 W_{\text{thr}}$, and stabilizes at a ~ 0.9 – 0.95 level up to a hundredfold increase above threshold. With decreasing focal length of the lens (to $F = 0.6 \text{ m}$) the dependence of the reflection coefficient on the excess above threshold is smoother, but at sufficiently high pump-pulse energy the reflection coefficient approaches the same level as for the long-focus lens, namely $R_w = 0.9$ – 0.95 (Fig. 1, curve 2). The energy balance was maintained in the entire range of excess above threshold, i.e., the sum of the energies of the transmitted and scattered pulses was equal to the pump-pulse energy; this is indirect evidence of the absence of collateral nonlinear effects.¹

A qualitative comparison of typical transverse structures of the pump and scattered-light beams shows them to be clearly in accord in both the near (Fig. 2a) and the far (Fig. 2b) zones. This indicates a high accuracy of the WFR in SMBS in compressed gases (see also Ref. 2). A quantitative measure of the accuracy of the WFR is the relative fraction χ of the power of that reflected-wave component in which the amplitude and phase distributions coincide with the corresponding distributions in the pump wave. The value of χ is^{6,7}

$$\chi = \left| \int \mathcal{E}_0 \mathcal{E}_1 ds \right|^2 / \int |\mathcal{E}_0|^2 ds \int |\mathcal{E}_1|^2 ds, \quad (1)$$

where \mathcal{E}_0 and \mathcal{E}_1 are the complex amplitudes of the incident and reflected waves, respectively.

The parameter χ is most useful for the description of the WFR of multimode light beams, but its calculation is also of interest for a quantitative estimate of the WFR accuracy for beams close to single-mode beams. To determine χ we must find the complex amplitudes \mathcal{E}_0 and \mathcal{E}_1 . The transverse distributions of the intensities of the light beams are obtained from photometry data. To determine the phase profile we use the fact that under experimental conditions the intensity distributions of the incident and reflected beams in the near and far zones are symmetrical and close to Gaussian, and the

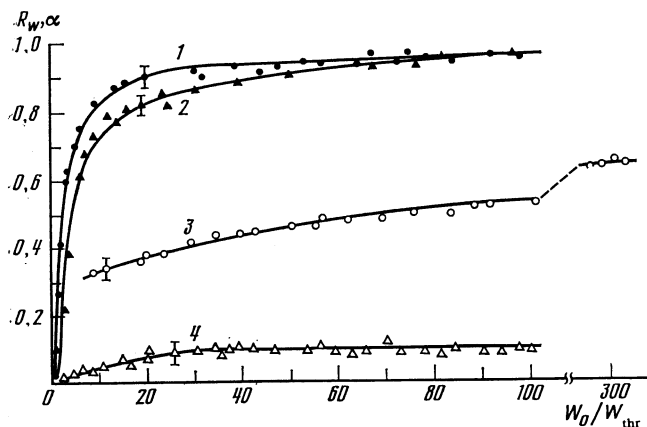


FIG. 1. Dependence of the reflection coefficient R_w (curves 1, 2, 3) and of the parameter α (4) on the excess W_0/W_{thr} above the SMBS threshold. 1— R_w of SF₆ SMBS mirror with lens focal length $F = 105 \text{ cm}$, 2— $F = 60 \text{ cm}$, 3— R_w of acetone SMBS mirror.

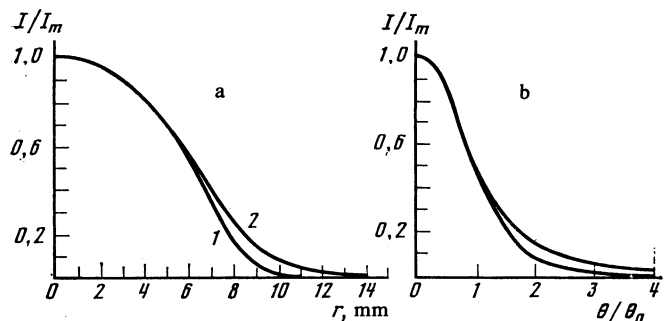


FIG. 2. Distribution of the intensities of the incident (1) and reflected (2) waves in the near (a) and far (b) zones.

corresponding divergences $\theta_0 = 6.8 \times 10^{-5} \text{ rad}$ and $\theta_1 = 7.1 \times 10^{-5} \text{ rad}$ differ little from the differential limit $\theta_d = 4/k_0 d_0 = 4.8 \times 10^{-5} \text{ rad}$, which is the same for both beams, since their radii in the near zone are practically the same. In this case it can be approximately assumed that the wave fronts of the incident and reflected light beams are spherical, i.e., in the paraxial approximation their phase is a quadratic function of the transverse coordinates. (If the higher-order aberrations of the wave front were substantial, the divergence of the light beams would exceed noticeably the diffraction limit and would increase drastically with broadening of their radius, e.g., as a result of saturation of the amplifiers, but this contradicts our experiment.) Approximating with sufficiently high accuracy the transverse distributions in the near and far zones by Gaussian curves, we can estimate the effective curvature radii of the wave fronts of the incident and reflected beams in the near zone, using the equation

$$R_{0,1}(0) = 2d_0 / (\theta_{0,1}^2 - \theta_d^2)^{1/2}. \quad (2)$$

Substitution of the measured values of d_0 , θ_0 , and θ_1 in (2) yields $R_0(0) = 540 \text{ m}$ and $R_1(0) = 580 \text{ m}$.

The phase factor under the integral sign in the numerator of (1) is equal to

$$\exp[ikr^2(R_0^{-1}(z) - R_1^{-1}(z))], \quad (3)$$

where $R_{0,1}(z)$ are taken in the plane of the measurement of the intensities I_0 and I_1 . (The values of $R_{0,1}(z)$ are expressed in terms of $R_{0,1}(0)$ in accord with the standard equations for a Gaussian beam.)

A direct numerical calculation of the integrals in (1) with allowance for (3) in real distributions of the amplitudes $I_0^{1/2}$ and $I_1^{1/2}$ has yielded the value of χ . According to measurements in the far zone, for angles smaller than $4\theta_0$ this value, averaged over different realizations, turned out to be 0.97 ± 0.01 . (The limit $4\theta_0$ on the photometry angle is due to the difficulty of recording on a single film the intensity distributions in a wide dynamic range; in the case of our experiment, registration within the angle range $4\theta_0$ was effected with a mirror wedge in a dynamic range ~ 200 .) Direct measurements of the energy fraction concentrated in the wings of the angle spectrum have shown, in addition, that outside the angle range $4\theta_0$ the relative energy of the incident radi-

ation is practically zero, while that of the incident radiation is about 2% (in the entire interval $R_w = 0.9-0.95$). Therefore, according to measurements in the far zone, the accuracy of the WFR in SMBS of single-mode light beam in SF₆ gas is $\chi_{f.z.} = 0.95 \pm 0.01$. The value of χ calculated from measurements in the near zone was found to be $\chi_{n.z.} = 0.93 \pm 0.01$. The mean value is thus²⁾ $\chi = 0.94 \pm 0.02$.

It must be noted that the quantity χ depends very little on small variations of the transverse profile of the light beam. Therefore, the inevitable photometry errors inherent in measurements by the focal-spot method and amounting to ~5-10% have practically no effect on the value of χ .

In the investigations of the energy and spatial characteristics of the radiation passing through the cell with the SF₆, we recorded both the total radiation energy $W_{0,out}$ as well (after correcting for the spherical curvature of the wave front) the energy $W'_{0,out}$ outside a cone with apex angle $10\theta_0$. The ratio $\alpha = W'_{0,out}/W_{0,out}$ of these energies as a function of W_0/W_{thr} is shown in Fig. 1 (curve 4). After the threshold was exceeded, the value of α increased monotonically, reaching approximately 10% at $W_0/W_{thr} = 20$, and next, just as the reflection coefficient, remained practically unchanged. The indicated behavior of the of α signifies in essence neither advanced breakdown nor even a pre-breakdown state is produced in SF₆. (Otherwise a strong negative defocusing lens would have to be produced in the focal region by the gas ionization, and this would increase the divergence of the radiation passing through the cell and hence lead to a substantial increase of α with increasing pump-wave power.)

The monotonic increase of the parameter α and its stabilization at a constant level (after the reflection coefficient reaches values $R_w \sim 0.9$) can be qualitatively explained by recognizing that a Stokes beam is subject to small-scale perturbations of the transverse profile. These weak perturbations interfere with the single-mode pump beam and excite an additional hypersound wave. Scattering of the strong wave from the hypersound wave leads to WFR of the indicated perturbations, i.e., to modulation of the pump wave.¹² The depth of this modulation, characterized by the parameter α , increases with increasing energy of the Stokes pulse. As R_w approaches unity, however, the value of α becomes stabilized, apparently because of the exhaustion of the pump wave and the decreases of the characteristic size of its interaction with the perturbations in the Stokes wave.

3. TEMPORAL EVOLUTION OF THE HYPERSONIC WAVE

To describe more accurately the weakening of the pump pulse as it enters the nonlinear medium we investigated the dynamics of the reflection of this pulse from the hyperpulse near the entrance into the cell. This was done by performing the following experiment. An additional cell C_1 , of length, $L = 0.3$ m, likewise filled with SF₆ at a pressure $p = 16$ atm, was placed ahead of the cell C_2 into which the pump beam was focused (Fig. 3). We measured the dependence of the power reflection coefficient on the time in the nonlinear-medium layer contained in cell C_1 . This was done by record-

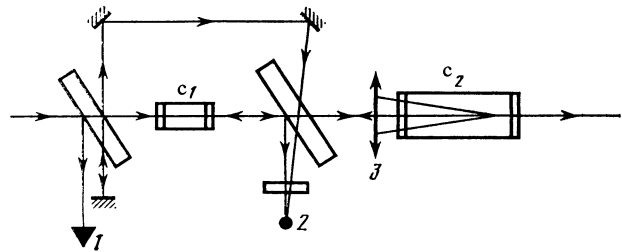


FIG. 3. Experimental setup for the investigation of time evolution of hypersound wave: 1—IMO-2, 2—coaxial photocell 15-km, 3—lens ($F = 105$ cm, C_1 —cell with SF₆ ($L = 30$ cm), C_2 —cell with SF₆ of length 100 cm.

ing the oscillograms of the powers $P_0(0,t)$ and $P_0(L,t)$ respectively of the pump pulses incident on and reflected from this cell. On the basis of these measurements we calculated the value

$$R(t) = [P_0(0,t) - P_0(L,t)] / P_0(0,t). \quad (4)$$

Figure 4 shows the time dependences of $R(t)$, with curves 1-3 obtained at $W_0(0)/W_{thr} = 60$ (1), 80 (2), 90 (3). The dashed lines a and b show $P_0(L,t)$ and $P_0(0,t)$ (for $W_0(0)/W_{thr} = 90$). With increasing pump-pulse energy, the maximum value of $R(t)$ increases, and with it the power reflection coefficient

$$R_w' = [W_0(0) - W_0(L)] / W_0(0),$$

while the energy $W_0(L)$ at the exit from the cell C_1 decreases:

$W_0(0)/W_{thr}$	60	80	90
$P_0(t)_{max}$	0.55	0.77	0.84
R_w'	0.4	0.64	0.7
$W_0(L), J$	0.54	0.43	0.4

It can be seen from the foregoing relations that the higher the pump-pulse energy the earlier the start of the formation of the hypersound wave in cell C_1 and the larger the growth rate (slope) of $R(t)$. In view of the nonstationary character of the SMBS, the fall-off rate of $R(t)$ is substantially less than the slope of the trailing end of the pump pulse $P_0(0,t)$ when the growth rate of $R(t)$ approximately equals the slope of the leading front of the pulse $P_0(0,t)$. In other words, notwithstanding the greatly weakened pump power at the end of the

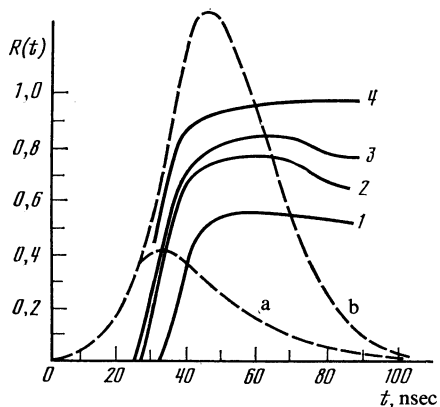


FIG. 4. Time dependence of the reflection coefficient $R(t)$ of cell C_1 for different ratios W_0/W_{thr} 1— $W_0/W_{thr} = 60$, 2—80, 3—90, 4—theoretical $R(t)$ dependence at $W_0/W_{thr} = 90$. Curves a and b show respectively the pulses at the exit and entrance of cell C_1 at $W_0/W_{thr} = 90$.

pump pulse, the hypersonic wave it excites jointly with the opposing Stokes pulse still exists.

The obtained experimental $R(t)$ plots can be compared with the theoretical ones calculated under the assumption that the coefficient of power reflection from cell C_2 is unity, and that there are no Fresnel losses in the optical elements between cells C_1 and C_2 . We use for this purpose the circumstance that the travel time of the light through the cell C_1 is negligibly short compared with the characteristic time scale of the change of the pulse shape. Since $R(t) = 1$ at the boundary of the cell C_1 , it can be easily noted that in this case the complex amplitudes \mathcal{E}_1 and \mathcal{E}_0 of the scattered and pump waves are equal in any plane of the C_1 volume. Since the waves interacting in cell C_1 are plane, the local extinction coefficient $\sigma = I_0^{-1} dI_0/dz$, which represents the relative change of the pump-wave intensity per unit length of the medium, is proportional to the hypersonic-wave amplitude. The latter, in turn, depends on the product of the wave amplitudes \mathcal{E}_0 and \mathcal{E}_1 , i.e., on the intensity I_0 . If we neglect the hypersonic damping, we note that

$$\sigma(z, t) = \frac{g}{T_2} \int_{-\infty}^t I_0(z, t) dt,$$

where g is the local growth rate per unit length and per unit intensity. Hence

$$\frac{dI_0}{dz} = \frac{g}{T_2} I_0 \int_{-\infty}^t I_0(z, t) dt, \quad \frac{dw_0}{dz} = \frac{g}{2T_2} w_0^2, \quad (5)$$

where

$$w_0(z, t) = \int_0^z I_0(z, t) dt.$$

Solving the last equation we get $I_0 = \dot{w}_0$, where

$$w_0(z, t) = w_0(0, t) [1 + (gz/2T_2) w_0(0, t)]^{-1}. \quad (6)$$

The coefficient of reflection from layer C_1 is equal to

$$R(t) = 1 - \exp\left\{-\int_0^z \sigma dz\right\}.$$

The result of the calculation by this formula, for incident pulse energy $W_0 = 90 W_{\text{thr}} = 135 \text{ J}$, is shown in Fig. 4 (curve 4). (The time for the theoretical curve is reckoned from the instant when the coefficient of power reflection from cell C_1 reaches³⁾ 50%.) We see that the theoretical (4) and experimental (3) curves are in approximate agreement, but only in the interval of the fast growth of $R(t)$. At the end of the pulse the experimental and theoretical plots diverge, since no account of the hypersonic damping was taken in the calculation.

The hypersonic relaxation time T_2 can be estimated from the following considerations. At the instant t_0 when $R(t)$ reaches a maximum the integral (over the layer length)

contribution to the hypersonic wave from the electric field

$$\sim \int_0^L I_0 dz$$

is balanced by the relaxation. The quantity

$$\int_0^L I_0 dz$$

depends in turn on the spatial distribution of $\sigma(z, t)$ at the preceding instants of time. Since the maximum of $R(t)$ and of

$$\int_0^z \sigma(z, t) dz$$

is reached directly past the section of fast growth of these values, i.e., after an interval in which the theoretical and experimental relations are approximately equal, it can be approximately assumed that

$$\int_0^z I_0 dz$$

is determined at the instant t_0 by the $\sigma(z, t)$ distribution calculated without allowance for the hypersonic relaxation. On this basis we can approximately estimate the relaxation time

$$T_2 = \left(\int_0^L \sigma(z, t) dz \right)_{\text{exp}} \left[\left(\frac{g}{T_2} \int_0^L I_0 dz \right)_{\text{theor}} \right]^{-1}, \quad t = t_0.$$

As a result we obtain $T_2 = 30 \text{ nsec}$, which is less than half the published values.¹³

Summing up, we can state that hypersonic excitation in nonstationary SMBS of focused single-mode light beams in compressed gases takes place first near the focus of the lens, and later in the plane ahead of the focus at the entrance to the cell, i.e., in the nonstationary case the characteristic boundary of the region of substantial weakening of the pump pulse power by reflection from the hypersonic shifts towards the source of the laser beam. As a result the power of the pulse passing through the focal constriction decreases drastically with time, thus contributing to avoidance of optical breakdown and to increasing the energy interval in which SMBS is realized. The shapes of the wavefronts of the hypersonic and of the pump beam are practically equal, and the WFR accuracy is $\chi = 0.94 \pm 0.02$. The distortions of the wave front of the radiation passing through the nonlinear medium are also relatively small.

4. TWO-PASS AMPLIFIER WITH NONSTATIONARY SMBS MIRROR

The near-unity values of the reflection coefficient R_W and of the accuracy χ of the WFR of an SF_6 SMBS mirror make it possible to use this mirror to attain high spectral

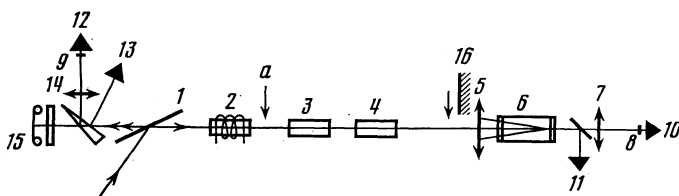


FIG. 5. Two-pass amplifier with nonstationary SMBS mirror: 1—thin-film polarizer, 2—Faraday cell, 3, 4—amplifiers, 5—lens ($F = 105 \text{ cm}$), 6—SMBS cell with SF_6 , 7—lens with $F = 80 \text{ cm}$, 8, 9—screens, 10—IMO-2, 14—lens with $F = 200 \text{ cm}$, 15—photcamera, 16—flat mirror.

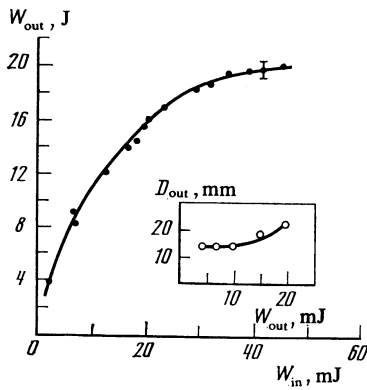


FIG. 6. Dependence of the output energy W_{out} of a two-pass amplifier on the input energy W_{in} . The inset shows the dependence of the diameter D_{out} of the emerging beam on its energy W_{out} .

brightness of the optical radiation at the output of a two-pass amplifier. We have investigated in this connection the system shown in Fig. 5. We measured the dependence of the output energy W_{out} of the two-pass amplifier on the input energy W_{in} (Fig. 6) in section *a* indicated in Fig. 5, as well as the dependence of the diameter D_{out} of the emerging beam on its energy (see inset of Fig. 6). The curvature of the outgoing-beam wave front causes its divergence to increase somewhat with increasing radius (owing to saturation of the amplifiers). For example, at a diameter $D_{out} \approx 14$ mm, when the saturation is small, the divergence (at the $1/e$ level) is $\theta_{out} = 7.1 \times 10^{-3}$ rad, while at $D_{out} = 23$ mm, when the saturation is substantial, the divergence $\chi'_{out} = 8.1 \times 10^{-5}$ rad. It is interesting to note that an estimate of the curvature radius by Eq. (2) yields for the two indicated cases the close values $R_{out} = 540$ m and $R'_{out} = 600$ m. This shows that in the amplifier-saturation regime the beam only increases in diameter but is not subject to phase distortions. When the SMBS mirror was replaced by a plane mirror, the exit intensity distribution remained the same as before in the far and near zones, i.e., in this case, too, the amplifiers introduced no phase distortions. A similar mirror substitution, however, starting with output radiation energy $W \approx 10$ J, caused self-excitation of the amplifiers, which limited the possibility of increasing the spectral brightness of the radiation.

In the presence of an SF₆ SMBS mirror, the spectral brightness $d^2I/\partial\omega\partial\Omega$ of the radiation at the output of the system of two amplifiers (using GLS-22 glass of 30 mm diam and 320 mm length) was 5×10^8 J/cm², approximately half the record value obtained earlier in Ref. 2. The energy density of the output radiation (at 50% filling of the amplifier aperture) was $w_{out} = 8$ J/cm², corresponding to a delivered

energy 0.12 J/cm³.

The authors thank the participants of the seminar headed by I. G. Zubarev for valuable remarks.

¹On the contrary, side effects seem to exist for SMBS in acetone: since there is no energy balance, R_w increases much more slowly as the threshold is exceeded (curve 3 of Fig. 1), and starting with 50- to 70-fold excess radiation with strongly inhomogeneous spatial field structure is mixed in with the directional SMBS radiation.^{4,5}

²If the quality of the WFR is estimated from the measured values of the parameter $h = [W_1(\varphi)/W_1(\infty)]/[W_0(\varphi)/W_0(\infty)]$ (Refs. 4, 8-10), where $W_{0,1}(\varphi)$ are the energies of the incident and reflected waves concentrated in some given angle φ , then for $\varphi \leq 1.5\theta_0$ we get ($1.5\theta_0$ is the angle that contains 80% of the energy of the incident radiation). At $\varphi > 1.5\theta_0$ the value of h increases and reaches 0.98 at $\varphi = 4\theta_0$. The difference between the values of h and χ is a consequence of their definitions. It is easy to realize reflection when $\chi \ll 1$ but $h \sim 1$, and conversely, as in our experiment, it may turn out that $h < \chi$ at $\chi \sim 1$ (the decrease of h compared with χ is due in this case to a well-known fact: the presence of a small, several percent in terms of energy, admixture of an uninverted component in the reflected wave causes strong modulation of the wave intensity).

³The parameter g/T_2 was assumed in the calculation to equal 2×10^5 cm/MW-sec. This value (with a spread $\sim 25\%$) was obtained by comparing the measured and theoretically calculated excitation threshold of nonstationary SMBS in focused beams.

¹B. Ya. Zel'dovich, V. I. Popovichev, V. V. Ragul'skii, and F. S. Faizullov Pis'ma Zh. Eksp. Teor. Fiz. **15**, 160 (1972) [JETP Lett. **15**, 109 (1972)].

²V. F. Efimkov, I. G. Zubarev, A. V. Kotov, A. B. Mironov, S. I. Mikhailov, and M. G. Smirnov Kvantovaya Elektron. (Moscow) **6**, 2031 (1979) [Sov. J. Quantum Electron. **9**, 1194 (1979)].

³V. F. Efimkov, I. G. Zubarev, A. V. Kotov *et al.*, Kvantovaya Elektron. (Moscow) **7**, 372 (1980) [Sov. J. Quantum Electron. **10**, 211 (1980)].

⁴K. V. Gratsianov, V. I. Kryzhanovskii, V. V. Lyubimov *et al.*, in: Obrashchenie volnovogo fronta izlucheniya v nelineinykh sredakh (radiation Wave-Front Reversal in Nonlinear Media), Inst. Phys. Probl. Press, Gorky, 1982, p. 143.

⁵M. V. Vasil'ev, V. G. Sidorovich, and N. S. Shlyaposhnikova Opt. Spektrosk. **54**, 651 (1983).

⁶V. I. Bespalov, A. A. Betin, and G. A. Pasmanik Padiofizika **20**, 791 (1977).

⁷B. Ya. Zel'dovich and V. V. Shkunov Kvantovaya Elektron. (Moscow) **4**, 1090 (1977) [Sov. J. Quantum Electron. **7**, 610 (1977)].

⁸N. G. Basov, V. F. Efimkov, I. G. Zubarev *et al.* Kvantovaya Elektron. (Moscow) **6**, 765 (1979) [Sov. J. Quantum Electron. **9**, 455 (1979)].

⁹Yu. V. Dolgoplov, Yu. F. Kir'yanov, S. B. Kormer, *et al.*, in: Obrshchenie volnovogo fronta opticheskogo izlucheniya v nelineinykh sredakh, (Optical-Radiation Wave-Front Reversal in Nonlinear Media), Inst. Phys. Probl. Press, Gorky, 1979, p. 117.

¹⁰V. I. Kryzhanovskii, V. A. Serebryakov and V. E. Yashin, Zh. Tekh. Fiz., **52**, 1356, (1982) [Sov. Phys. Tech. Phys. **27**, 825 (1982)].

¹¹V. V. Gil'denburg Nelineinye volny: rasprostraneniye i vzaimodeystvie. (Nonlinear Waves: Propagation and Interaction) M.: Nauka, p. 87, (1981).

¹²V. I. Bespalov, A. A. Betin, G. A. Pasmanik and A. A. Shilov Pis'ma Zh. Tekh. Fiz., **5**, 242, (1979) [Sov. Tech. Phys. Lett. **5** 97 (1979)].

¹³V. F. Efimkov, I. G. Zubarev, A. V. Kotov, *et al.*, Zh. Eksp. Teor. Fiz. **77**, 526 (1979) [Sov. Phys. JETP **50**, 267 (1979)].

Translated by J. G. Adashko